pK_a of the mRNA Cap-Specific 2′-*O*-Methyltransferase Catalytic Lysine by HSQC NMR Detection of a Two-Carbon Probe†

C. Li and P. D. Gershon*

Department of Molecular Biology and Biochemistry, University of California—Irvine, Irvine, California 92697-3900

Received August 28, 2005; Revised Manuscript Received November 23, 2005

ABSTRACT: We have characterized the side chain pK_a for a single lysine analogue within a 316-residue protein containing 21 lysines and 1678 carbon atoms at natural isotope abundance. To do this, the single reactive cysteine of a K175C mutant of VP39 (the mRNA cap-specific 2′-*O*-methyltransferase from vaccinia virus) was modified to *S*-(*β*-aminoethyl)cysteine (*γ*-thialysine) using freshly prepared (^{13}C)aziridine at room temperature. Modification was accompanied by the rescue of catalytic function at high specific activity. After the fastidious removal of the noncovalently protein-bound aziridine self-polymer using a novel chelating dialysis procedure, signals were monitored by HSQC NMR. Appropriately pH-shifting HSQC NMR peaks were identified in the (^{13}C)aziridine-modified enzyme, corresponding to detection of the two covalently attached (^{13}C)thioethylamino atoms. The identification was strengthened by comparison with the positions and pH shifts of spectral peaks for tripeptide controls, a small molecule aziridine self-polymer mimetic, and a cysteine-minus control enzyme. pH titration of the modified protein indicated an apparent pK_a of 8.5, consistent with a perturbed pK_a for the catalytic lysine and a model in which the surrounding charged groups direct the lysine *ϵ*-amino pK_a via both local electrostatic environment and orbital directionality.

Chemical modification rescue of enzymes containing a catalytic lysine by lysine → cysteine mutation followed by site-specific S-aminoethylation of the cysteine side chain to the unnatural residue *γ*-thialysine (which is identical in molecular structure other than replacement of the *γ*-CH_2 with isosteric S) was first described by Smith et al. (*1*) and has proven useful in the investigation of enzyme mechanisms (*1*−*15*). Although this approach provides a potential route for the site-specific incorporation of an isotope-enriched ethylamino group, for the monitoring of the catalytic center microenvironment by NMR, such an application has not, to our knowledge, been reported to date. For such an application to be effective, several conditions would need to be met, namely, (a) the presence of only a single reactive site (cysteine) within the protein, (b) fastidious removal of isotope-enriched unreacted reagents and side products, (c) modification of the protein with only the monomeric form of *S*-ethylamine, and (d) proof that the NMR signal present after modification and cleanup procedures arose from the ethylamine moiety covalently attached to protein, at the target site.

Vaccinia virus protein VP39 is an RNA 2′-*O*-methyltransferase, catalyzing transfer of the methyl group from *S*-adenosylmethionine to the 2′OH of the 5′-most transcribed nucleotide of N7mG-capped RNA. Active forms of the protein possess at least 21 lysine residues, rendering the NMR spectroscopy of uniformly stable heavy-isotope-labeled protein impractical for the purpose of monitoring individual side chains. Here, we demonstrate the site-specific chemical modification rescue of VP39 at an essential catalytic lysine, addressing the conditions outlined above, and demonstrate pK_a monitoring of the rescued side chain by HSQC NMR.

MATERIALS AND METHODS

Materials. (^{13}C)-1,2-Dibromoethylene was purchased from Cambridge Isotope Labs Inc. Potassium phthalimide was obtained from Sigma-Aldrich Inc.

Generation of VP39 Mutant C272S/K175C/R209K. A K175C mutation was introduced into a plasmid containing the coding sequence for GST-VP39-C272S (*16*) using the Chameleon double-stranded site-directed mutagenesis kit (Stratagene) according to the manufacturer's instructions. Briefly, template was co-annealed with mutagenic primer and a *Pst*I/*Sac*II toggle primer followed by primer extension/ligation, transformation of XLmutS cells, and overnight growth of cells, plasmid preparation and *Pst*I digestion, retransformation, colony screening, and sequencing. The resulting insert was recloned as an *Nco*I*Hin*dII fragment in plasmid pET30a (Novagen Inc.), followed by introduction of the R209K mutation as a commercial service (MCLAB, San Francisco), followed by sequencing of the mutant insert.

Expression and Purification of VP39 Mutant C272S/K175C/R209K. VP39-C272S/K175C/R209K was expressed and purified as outlined for the mutant K175C (*17*), except that the expression time was 4 h.

Methyltransferase Assay. The short RNA substrate m^{7}G-(5′)pppGpApApA was generated by in vitro transcription as

† This work was supported by National Science Foundation Grants MCB-9604188 and MCB-0091260.

* Corresponding author. Phone: 949-824-9606. Fax: 949-824-8551. E-mail: pgershon@uci.edu.

10.1021/bi051736h CCC: $33.50
Published on Web 12/27/2005

described (*17*) except that N^7mG(5′)pppG (NEB) had natural carbon abundance and thioATP was replaced with ATP. The cap-specific 2′-*O*-methyltransferase assay was performed as described (*18*), with reactions incubated for 60 min at 30 °C. Dried 25% polyacrylamide gels were exposed to a tritium storage phosphor screen (Fuji) which was then scanned and electronically imaged using a Molecular Imager FX Pro Plus (Bio-Rad).

Synthesis of Aziridine and (^{13}C)Aziridine. (A) 2-Bromoethylphthalimide. Five grams of $BrCH_2CH_2Br$ or $Br^{13}CH_2{}^{13}CH_2Br$ (dibromoethylene) was dissolved in 40 mL of anhydrous acetone in a 100 mL triple-neck flask with a magnetic stirring bar. Addition of 5 g of potassium phthalimide was followed by reflux for 24 h under argon. The resulting mixture was filtered to remove solid potassium bromide residue. The 2-bromoethylphthalimide product was separated from unreacted dibromoethylene in the same solution by fractional distillation. ^{1}H NMR (500 MHz): 3.4827−3.4504 (m), 3.7845−3.7711 (m), 3.9745−3.9553 (m), 4.2743−4.2415 (m), 7.88891 (q), 7.7600 (q)−7.7355. ^{13}C NMR (500 MHz): 28.506 (d), 39.632 (d). (TMS as 0 ppm). Fractionated 2-bromoethylphthalimide product was dried. Stepwise yield: 80%.

(B) 2-Bromoethylamine−HBr. 2-Bromoethylphthalimide was hydrolyzed by dissolving in concentrated (48%) HBr and then incubating at 138 °C. After 10 h, the mixture was filtered and the filtrate extracted three times with diethyl ether. ^{13}C NMR (500 MHz): 31.0073, 30.7114 (J_{CC} = 36.98 Hz), 44.0678, 43.6943 (DSS as internal reference). 2-Bromoethylamine−HBr was recovered from the aqueous phase by evaporation under reduced pressure. Stepwise yield: 90%.

(C) Aziridine. Aziridine was synthesized by hydrolysis of 2-bromoethylamine−HBr in NaOH as described (*19*). ^{1}H NMR (500 MHz): 1.78314, 1.45175 (J_{CH} = 165.7 Hz). ^{13}C NMR (500 MHz): 20.0053. These NMR data supported ^{13}C-labeled aziridine as the product.

Tripeptide Synthesis and Modification. Tripeptides ACW and AKW were synthesized manually by standard solid-phase FMOC chemistry. AKW was cleaved from the support using 98% TFA[1]/2% triisopropylsilane. For synthesis of AC_mW (where C_m represents cysteine modified to γ-thialysine), the protecting monomethyltrityl group on the cysteine side chain of ACW was removed using 5% TFA/2% triisopropylsilane in dichloromethane, and the support-bound ACW was washed at least three times with DMF to eliminate the TFA. Support-bound ACW was then mixed with freshly prepared aziridine (at a concentration of ∼1−∼10 mM in DMF). After 6 h at room temperature, AC_mW was cleaved from the support as described above. Following cleavage, AKW and AC_mW were precipitated with cold diethyl ether, washed once with diethyl ether, dissolved in water, and then lyophilized. They were then each purified by C18 column chromatography (Waters, Inc., model 2525 binary gradient module, 515 HPLC, model 2996 diode array detector, and column fluidics organizer) running a 15 min gradient of 4−20% CH_3CN in 0.1% TFA with online LC-MS monitoring (Micromass ZQ micro API benchtop single quadrupole mass spectrometer/MassLynx 4.0 software). Fractions corresponding to target molecules were lyophilized to dryness. Average *m*/*z* ($[M + H]^+$), expected/observed: AKW, 403.222/403.390; ACW, 378.136/378.190; AC_mW, 421.136/421.20.

Protein Chemical Modification Rescue. Ni-NTA column fractions containing the most pure and abundant VP39-C272S/K175C/R209K [typically at a concentration of ∼75−100 μM in a volume of 2 mL of 50 mM sodium phosphate and 250 mM NaCl (pH 7.4) (*17*)] were mixed with DTT (∼20-fold molar excess over protein thiol) and then incubated at room temperature for 4 h under argon. After 2 mL of 0.5 M sodium phosphate (pH 8.5) was added, aziridine was added stepwise over the subsequent 6 h. Free thiol concentration was monitored during the reaction by derivatization with 5,5′-dithiobis(2-nitrobenzoic acid) (*20*). The reaction was quenched by addition of excess DTT followed by extensive dialysis against (sequentially) buffer A (2 mM HEPES, 0.2 M NaCl, pH 8.0), buffer B (2 mM HEPES, 0.1 mM $NiSO_4$, 0.2 M NaCl), two changes of buffer A, buffer C (2 mM HEPES, 0.1 mM EDTA, 0.2 M NaCl, pH 8.0), and then two changes of buffer D (25 mM sodium phosphate, 0.2 M NaCl, pH 6.4). The resulting protein was concentrated by ultrafiltration (Centricon; Millipore Inc.).

VP39 mutants were supplemented with Tris-HCl (pH 7.8) to 100 mM and then with protease Arg-C (Roche Applied Science) at a substrate:protease mass ratio of 50−100:1, followed by incubation at 37 °C for 3−6 h. The resulting peptides were desalted using C18 Zip-Tips according to the manufacturer's instructions (Millipore Inc.), then mixed (1:1 v/v) with cyano-4-hydroxycinnamic acid matrix [Sigma-Aldrich Inc., freshly dissolved at 10 mg/mL in 50:50:0.1 (v/v) CH_3CN:H_2O:TFA], then dried on ground steel MALDI target plates, and analyzed by MALDI-TOF (Autoflex; Bruker Daltonics Inc.) in reflector mode.

NMR Spectroscopy. All NMR spectra were acquired at a temperature of 25 °C. Tripeptides were dissolved to a concentration of 10−40 mM in 0.2 M NaCl and 25 mM sodium phosphate buffer (pH 6.4) containing 10% D_2O. Protein VP39-C272S/K175C/R209K was at a concentration of 0.15 mM in this buffer. For tripeptides and protein, upward pH titrations were carried out by the stepwise addition of 2 M NaOD in D_2O (2−4 μL per pH point) with gentle mixing. The pH was monitored using a pH microprobe (model MI-710; Microprobes, Inc.) immediately before and immediately after collecting data, and the average pH was taken to be the actual value. TETA was dissolved in 25 mM sodium phosphate and 0.2 M NaCl (pH >11.0), and the pH was downward titrated by the stepwise addition of 2 M HCl. After each pH reading, the pH microprobe was rinsed with chromate and then water.

Tripeptide and TETA spectra were acquired using an 800 MHz instrument (Varian Unity Inova; UC−Irvine) with a triple resonance HCN6157 probe and *x*, *y*, *z*-pulsed field gradient. For assignment purposes, DQFCOSY spectra were acquired at the starting pH (pH 6.4) with a data matrix of 256 (t_1) complex pairs. Prior to the standard DQFCOSY pulse sequence, Watergate was used for water suppression (during the relaxation delay period, d_1 = 1.3 s). The spectral width was 9000 Hz in both dimensions. FID1 were multiplied with a sine-square-bell window function in both directions. DQFCOSY spectra were recorded over a 6−10 h period.

[1] Abbreviations: PEI, poly(ethylenimine); TFA, trifluoroacetic acid; DMF, dimethylformamide; DTT, dithiothreitol; HEPES, *N*-(2-hydroxyethyl)piperazine-*N*′-2-ethanesulfonic acid; TETA, triethylenetetramine.

For 2D [^{13}C,^{1}H]-HSQC spectroscopy of tripetides and TETA, 64 × 1024 data matrices in complex data points in the time domain were acquired with 16 transients for each FID. H_2O signals were suppressed using Watergate. Relaxation delay between scans (d_1) was 1.5 s. Spectra were obtained with sweep widths in t_1 and t_2 of 12001 and 14078 Hz, respectively. Linear prediction to 128 complex points in the t_1 dimension and cosine-square-bell window functions in both t_1 and t_2 dimensions were used before Fourier transformation. The final spectrum contains 256 × 2048 data points. Chemical shifts (δ) were calibrated relative to DSS. For each pH titration, one data set was recorded per pH point (corresponding to 8−10 data sets in all).

Protein NMR 2D [^{13}C,^{1}H]-HSQC spectra were acquired using Bruker Avance 600 or 800 MHz NMR spectrometers (University of Houston) with a ^{1}H/^{13}C/^{15}N TXI probe and *z*-pulsed field gradient. The pulse sequence was as for tripetides and TETA (above) except $d_1 = 0.5$ s. A total of 64 × 1024 data matrices in complex data points in the time domain were acquired with 720 transients for each FID. H_2O signals were suppressed using Watergate. The scalar evolution delay was 7.14 ms. Recovery delay between scans was 0.5 s. The carriers of ^{1}H and ^{13}C channels were set to 4.7 and 46 ppm, respectively. The spectral widths of ^{1}H and ^{13}C were 11160 and 8048 Hz, respectively. Linear prediction to 128 complex points in the t_1 dimension and cosine-square-bell window functions in both t_1 and t_2 dimensions were used before Fourier transformation, and the final spectrum contained 256 × 2048 data points. δ were calibrated according to DSS.

Curve Fitting. Since the exchange rates of protons from a primary amino group are fast compared to the observed chemical shifts (δ_{obs}) leading to NMR signal coalescence, δ_{obs} was taken to be a weighted average of chemical shifts attributable to the protonated (δ_{H^+}) and unprotonated (δ_{H^0}) forms (*21*). Our titration data were therefore fit to a modified version of the Hill equation, namely, eq 2 from ref *21*: $(\delta_{H^+} - \delta_{obs})/(\delta_{H^+} - \delta_{H^0}) = K_a^n/(K_a^n + [H^+]^n)$, where $(\delta_{H^+} - \delta_{obs})/(\delta_{H^+} - \delta_{H^0})$ is the fraction of molecules with a neutral amino group, K_a is the dissociation constant, and n is the Hill coefficient.

Rearranging:

$$\delta_{obs} = \delta_{H^+} - (\delta_{H^+} - \delta_{H0})/(1 + ([H^+]^n/K_a^n)) \qquad (1)$$

where δ_{obs} = ordinate (y) on plots of pH vs δ. Now, let δ_{H^+} (asymptotic value on the ordinate corresponding to full protonation) = K0, and $\delta_{H^+} - \delta_{H^0}$ (asymptote-to-asymptote span on the ordinate corresponding to the full change in protonation state) = K1, then eq 1 becomes $y = K0 - (K1/(1 + (K_a^n/[H^+]^n)))$. Since $K_a = 10^{-pK_a}$ and $[H^+] = 10^{-pH}$, then $y = K0 - (K1/(1 + 10^{n(pH-pK)}))$. Now, let p$K$ = K2, n (Hill coefficient) = −1/K3, and pH = x (abscissa on plots of pH vs δ), then $y = K0 - (K1/(1 + 10^{-(x-K2)/K3}))$. Nonlinear least-squares fitting of data to this sigmoidal function was performed using the program Igor Pro (version 5.03; Wavemetrics, Inc., Lake Oswego, OR). Statistical uncertainty (error) for the coefficient values was estimated by Igor Pro from the inverse of the Hessian matrix and the residuals.

Molecular Graphics. Molecular graphics were rendered using RasMol (*22*) and VMD (*23*), with PDB file 1av6 (*24*).

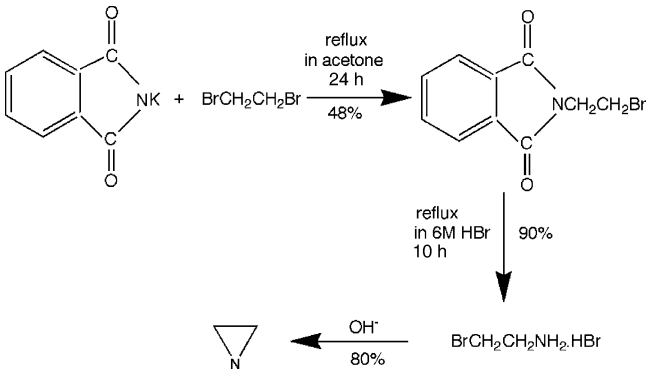

FIGURE 1: Synthesis of aziridine. For details see Materials and Methods.

RESULTS

To more fully understand the catalytic mechanism of the vaccinia virus mRNA cap-specific 2′-*O*-methyltransferase (VP39), we chose to determine the pK_a of lysine 175, located within the methyltransferase catalytic center. Since there was no obvious reporter group method (such as Schiff base formation) for this enzyme, we turned to direct pK_a measurement by NMR. Our strategy was to substitute lysine 175 with a cysteine in the context of a cysteine-minus variant of VP39 and then rescue to γ-thialysine using a ^{13}C-enriched version of either 2-bromoethylene−HBr or ethyleneimine (aziridine), thereby restoring full enzymatic activity and simultaneously incorporating ^{13}C/^{15}N stable heavy isotopes into the side chain. The apparent pK_a for the labeled side chain would be elucidated by pH titration with HSQC NMR monitoring.

Since 2-bromoethylamine has commonly been used for chemical modification rescue of cysteine to γ-thialysine (*1*, *3*−*15*, *25*), commercially prepared 2-bromoethylamine was tested for modification of VP39-C272S/K175C/R209K, followed by Arg-C protease digestion and MALDI-TOF analysis. The estimated extent of target site modification (∼64%; data not shown) was within the range observed by others with a variety of other proteins (*1*, *3*, *5*−*8*, *12*, *13*, *15*, *25*), and spurious modifications were not observed in MALDI-TOF spectra (data not shown). However, to achieve this level of modification, overnight reaction at 37 °C was required which, under the buffer and reagent conditions employed, led to considerable protein loss through aggregation.

To facilitate briefer and milder reaction conditions, we tried using aziridine [a derivative of 2-bromoethylamine (refs *26*−*28* and references cited therein)] as the modification reagent, under the assumption that it may be inherently more reactive than 2-bromoethylamine due to internal bond strain. A potential disadvantage in the use of aziridine, however, might be its potential to self-polymerize in aqueous incubations (*29*−*31*). To minimize storage time, aziridine was therefore synthesized and purified in-house, according to the scheme shown in Figure 1. Both freshly prepared and stored aziridine were tested for self-polymerization by LC-MS (data not shown). Self-polymerization was significant during storage at room temperature and could also be detected after −80 °C storage (data not shown).

Modification efficiency and product homogeneity were tested using, as an assay target, the tripeptide ACW (whose

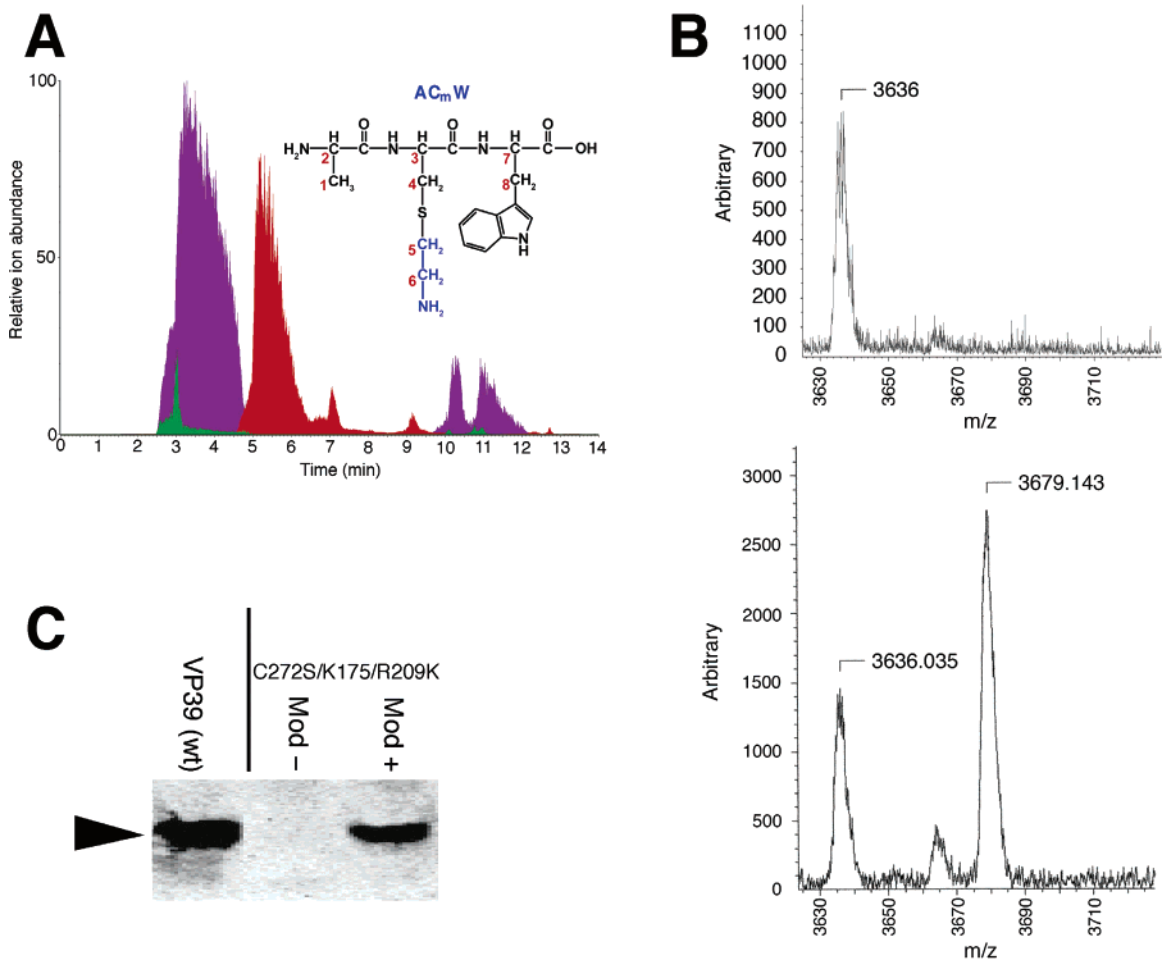

FIGURE 2: Polypeptide modification by aziridine. (A) On-resin modification of tripeptide ACW with freshly prepared (less than 24 h old) aziridine (synthesized with natural abundance isotopes). Tripeptide synthesis, cleavage from the resin, and deprotection were followed by C18 column purification of the resulting, crude reaction mixture with LC-MS monitoring. Shown superimposed are the extracted ion chromatograms for unmodified tripeptide (red, *m*/*z* 378), aziridine monomer-modified peptide (purple, *m*/*z* 421; inset molecule), and aziridine dimer-modified peptide (green, *m*/*z* 464). Minor products such as metal cation adducts of the three ions (not shown) were also detected, whose fractional abundances were equivalent for each the three species shown here. (B) Modification (4 h, room temperature) of VP39-K175C protein with freshly prepared aziridine (synthesized with natural abundance isotopes) followed by protease Arg-C digestion and MALDI-TOF analysis. Upper panel: Unmodified VP39-C272S/K175C/R209K [*m*/*z* 3636 peak is unmodified Arg-C peptide GGNEPSTADLLSNYALQNVMISILNPVASSL**C**WR (positions 144−177 in the wild-type sequence)]. Lower panel: After aziridine modification. The aminoethyl-modified peptide is 43 Da heavier. By integration of the areas under the peaks, it was estimated that 66.7% of the protein in the preparation was modified in this reaction (albeit that MALDI-TOF analysis may not be entirely quantitative). The minor peak at *m*/*z* 3665 appeared in both unmodified and modified spectra and was thus disregarded. (C) Methyltransferase activity of wild-type VP39 and the unmodified and modified C272S/K175C/R209K mutant. The arrow points to methylated substrate RNA.

sequence mimics that around the target single cysteine in VP39-K175C but with an L → A substitution due to concerns about peptide solubility). On-resin modification of ACW with freshly prepared aziridine at room temperature was efficient. At the conclusion of the reaction, an estimated 68.7% of the preparation was target site-modified with aziridine monomer (Figure 2A). Only ~5.3% of reaction products were aziridine dimer-modified, and higher order aziridine multimer-modified forms were barely detectable (Figure 2A).

Intact VP39-K175C protein was then incubated with the freshly prepared aziridine in a 4 h, room temperature reaction. The extent of target site modification at the conclusion of the reaction was estimated to be ~66.7% (Figure 2B). Although this was equivalent to the modification level achieved in an overnight incubation using 2-bromoethylamine at 37 °C (above), protein losses due to aggregation during the modification reaction were, notably, negligible in the lower temperature/shorter duration reactions employed for aziridine. Specific off-target modifications with aziridine were not detected though their occurrence in trace amounts could not be entirely discounted. Whereas unmodified VP39-C272S-K175C-R209K had no detectable methyltransferase activity, the modified protein was active (Figure 2C), exhibiting 20−30% of the specific catalytic rate of wild-type VP39 (data not shown).

To demonstrate whether there was a distinct spectral signature for the aminoethyl portion of aziridine-modified ACW (AC$_m$W), a control tripeptide AKW (in which the lysine aminoethyl group is attached to a carbon) was synthesized and purified. The two tripeptides, along with the small-molecule polymer mimetic TETA [$NH_2CH_2CH_2(NHCH_2CH_2)_2NH_2$] (in which the terminal aminoethyl groups are attached to nitrogens), were examined by NMR. After elucidating couplings within each of the three molecules by DQFCOSY leading to the assignment of all carbons in each

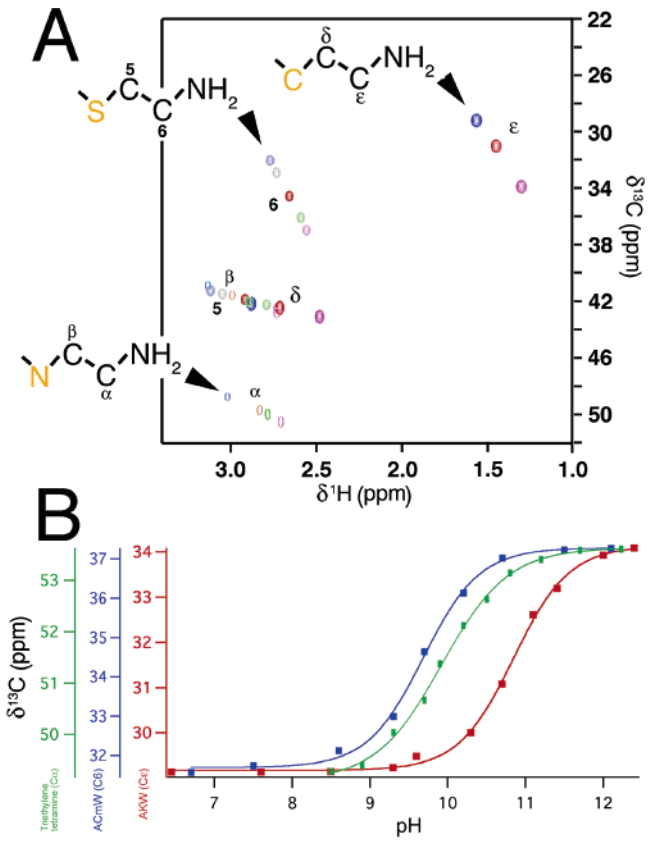

FIGURE 3: pH titration of AKW (mimetic of LKW, the sequence of VP39 around K175), AC_mW (γ-thialysine mimetic of AKW), and triethylenetetramine [$NH_2CH_2CH_2(NHCH_2CH_2)_2NH_2$]. (A) Superimposed HSQC NMR spectra acquired at pH values representing asymptotic and intermediate points in the titration of each tripeptide. For AC_mW carbons 5 and 6 (numbered according to Figure 2A inset), blue = pH 8.6, gray = pH 9.3, red = pH 9.7, green = pH 10.2, and mauve = pH 10.7. For AKW lysine carbons ϵ and δ (standard lysine nomenclature), blue = pH 9.6, red = pH 10.7, and mauve = pH 12.0. For triethylenetetramine carbons α and β (representing the amino-adjacent and Cα-adjacent carbons, respectively), blue = pH 7.47, red = pH 9.3, green = pH 9.96, and mauve = pH 11.7. (B) Plots (δ vs pH) showing the complete titrations including the subset shown in panel A for AC_mW (C6), AKW (Cϵ), and TETA (Cα). For each of the two tripeptides, indistinguishable curve fits and apparent pK_a values were obtained irrespective of which of the two aminoethyl carbons was monitored (carbon 5/6 or δ/ϵ for AC_mW and AKW, respectively; data not shown). It was later determined that tripeptide LKW, the bona fide mimetic of the sequence around position K175 of the VP39 sequence, was also soluble, and titration of this control peptide was identical to that of AKW (data not shown).

molecule (data not shown), they were each subjected to pH titration with HSQC NMR monitoring of the two aminoethyl carbons. The superimposed HSQC NMR spectra (Figure 3A) demonstrated highly distinct signatures for each compound, indicating that aziridine covalently attached to protein thiols is distinguishable from potential artifactual signals arising from either lysine or amino-derivatized protein.

In addition to their distinct spectral signatures, the three aminoethyl derivatives exhibited distinct pK_a values (Figure 3B). The pK_a of the ϵ-NH_2 group of free γ-thialysine has been reported to be almost 1 pH unit lower than that of free lysine [10.53 and 9.52 for free lysine and free γ-thialysine, respectively (*32*)]. To our knowledge however, the pK_a of the γ-thialysine side chain in the context of a polypeptide chain has not been reported. Curve fitting to plots of δ vs pH (Figure 3B) indicated apparent pK_a values of ~10.85 and ~9.68 for the side chain amino groups of AKW and AC_mW, respectively. Thus, although the solution pK_a values for the side chain amino groups were apparently elevated slightly for both lysine and γ-thialysine upon incorporation into an equivalent tripeptide context (by 0.32 and 0.16 pH unit, respectively), the apparent pK_a difference (~1.01−1.17 pH units) was maintained. This indicated that, although the absolute pK_a of the aminoethyl group was dependent upon covalent context (whether S- or C-coupled), a context-dependent polarizability (free amino acid vs tripeptide) was maintained for the amino group irrespective of covalent context. The latter factor was considered to adequately validate use of γ-thialysine as a covalent p*K* probe in intact proteins. Curve fitting to the TETA titration indicated a p*K*-amine of 9.94 (Figure 3B) that was distinguishable from the compound's p*K*-imine of 6.53 (data not shown).

For pK_a determination of modified intact proteins by HSQC NMR, aziridine enriched at both ^{13}C's (which was not commercially obtainable) was prepared as described above (Figure 1) and then used immediately for modification of VP39-C272S/K175C/R209K. Acceptable levels of correctly targeted protein modification were achieved using this reagent (Figure 4A shows an estimated level of 40.1%). Although the protein contains an additional cysteine at position 178, this cysteine is profoundly unreactive (*33*, *34*).

Albeit that the profiles of Arg-C peptides from the modified and unmodified proteins were essentially indistinguishable in MALDI-TOF spectra, with the exception of the target-containing peptide (Figure 4A; data not shown), MALDI-TOF spectra of intact VP39-C272S/K175C/R209K protein showed an average modification-dependent increase by ~3250 *m*/*z*, which corresponds to the mass of a polymer possessing ~72 aziridine monomer units (Figure 4B). Manifestly, the modified protein was associated with tightly noncovalently bound (^{13}C)aziridine-based self-polymer whose "stripping" from the protein would be necessary in order to avoid significant challenges in later HSQC spectral interpretation. Since the aziridine self-polymer presumably resembled PEI, a dialysis procedure was developed that exploited PEI's metal-chelating properties. This procedure was successful in returning the apparent molecular weight of protein, after the modification reaction, to the predicted molecular weight (Figure 4B) in a manner that was absolutely dependent upon the metal ion/chelation steps (data not shown). Figure 4C shows superimposed HSQC spectra for modified VP39-K175C/C272S protein before and after chelating dialysis (the spectrum shown after dialysis representing a 176-fold greater number of scans than that from before). The intensities of some spots (such as that marked "P" for "polymer") decreased or disappeared after dialysis, pinpointing their source as noncovalently bound material (presumably free aziridine self-polymer). Due to the scan-number difference between the two spectra, the extent of decrease was far greater than it would appear in Figure 4C. For other peaks (such as that marked "C" for "covalently bound") intensities were undiminished (they appear to increase in intensity due to the difference in scan number between the "before" and "after" spectra), identifying their source as covalently bound material. The signal marked C corresponds to the signal in Figure 3A arising from the (^{13}C)aminoethyl carbon atom covalently coupled to the

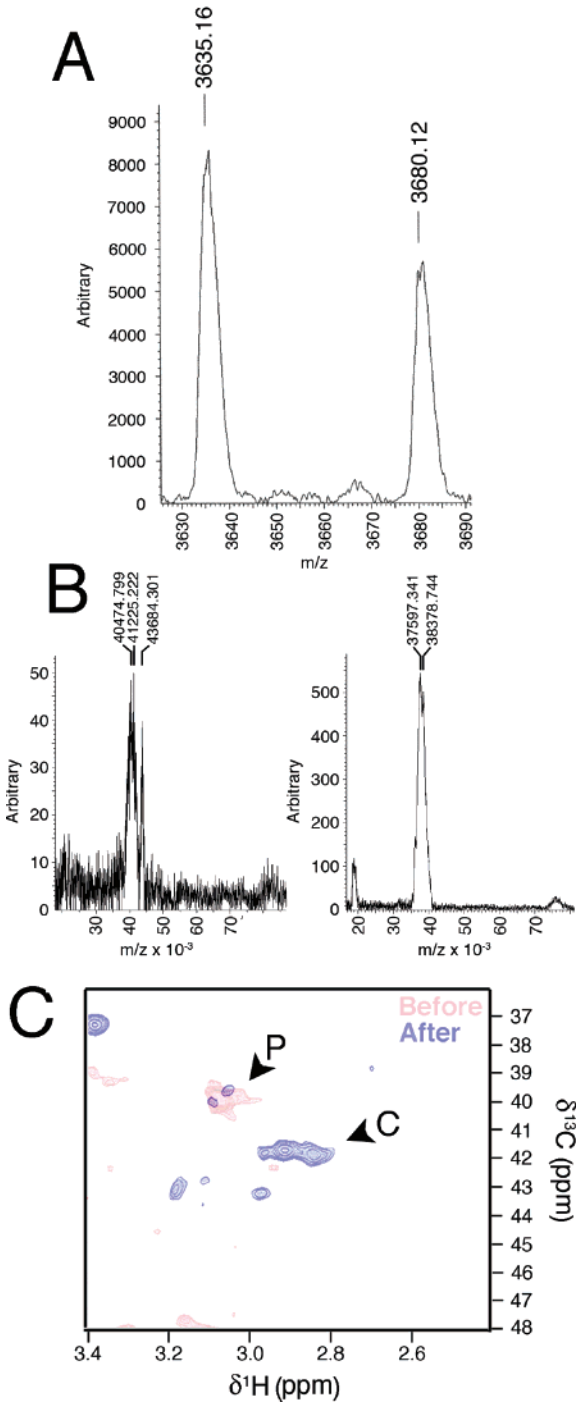

FIGURE 4: Modification of VP39-C272S/K175C/R209K with fresh (^{13}C)aziridine, followed by removal of self-polymerized aziridine by chelating dialysis. (A) Arg-C digestion followed by MALDI-TOF analysis. The 45 Da heavier form corresponded to the (^{13}C)-aminoethyl-modified peptide. It was estimated that, in this experiment, 40.1% of the protein in the preparation was modified (albeit that MALDI-TOF analysis may not be entirely quantitative); ≤5% of the aziridine was dimerized (data not shown). (B) Left: MALDI-TOF spectrum of aziridine-modified VP39-C272S/K175C/R209K directly after modification. The observed centroid *m/z* was higher than that predicted for the protein by ~3 kDa (~7−8%). Right: As left, except directly after the chelating dialysis procedure. (C) Change in HSQC/COSY spectrum for (^{13}C)aziridine-modified VP39-K175C/272S before (red, 4 scans) and after (blue, 704 scans) chelating dialysis (spectra superimposed). Spectra were acquired at pH 6.4. P (arrowed) is the most prominent signal that is lost during dialysis (presumed to be the noncovalently bound PEI polymer; see text). C is the most prominent of the signals that did not decrease during dialysis (covalently bound material).

attacking protein nucleophile (Figure 3A).

Aziridine-modified, dialyzed VP39-C272S/K175C/R209K was next pH-titrated, monitoring by HSQC at each pH step. Figure 5A shows the raw HSQC spectra obtained at five distinct pH values, superimposed. To more clearly identify the signal from the covalently attached (^{13}C)aminoethyl, several levels of data filtering were applied to the superimposed spectrum set. First, foldback signals were manually removed (Figure 5B). The spectrum set of Figure 5B was then compared with the spectra of Figure 4C to identify coinciding signals between the two experiments. The two strongest signals in Figure 5B (P and C) corresponded to P and C in Figure 4c (described above). The next most abundant signals in the spectrum set of Figure 5B shifted progressively with pH (shown connected with black lines). These were the only clearly observable signals in Figure 5B that shifted progressively with pH.

Figure 5C is a further edited version of Figure 5B in which P [which was identified as noncovalently bound material (Figure 4C) and which showed no obvious titration with pH] has been manually edited from the spectrum set. In addition, black, orange, and cyan rings in Figure 5C indicate the pH-dependent signals from carbons 5 and 6 of the AC_mW tripeptide, lysine carbon δ of the AKW tripeptide, and carbon β of triethylenetetramine, respectively (positions transposed from Figure 3A). Manifestly, the signals in Figure 5C corresponding to C (Figure 5B) arise from the attack upon (^{13}C)aziridine of nucleophile(s) in the protein which cannot be identified from these signals but which would include the K175C thiol, and/or endogenous lysine with carbon at natural abundance. Perhaps most interestingly, however, the signals in Figure 5C corresponding to those in Figure 5B that shifted progressively with pH (connected with black lines) corresponded precisely with the pH titration of AC_mW tripeptide carbon 6 (Figure 3A, the latter being transposed to Figure 5C as black circles) but not with the pH titration for either AKW (carbon ϵ) or TETA (carbon α) (Figure 3A). Thus, the black line-linked signals in Figure 5B,C were clearly identified as arising from (^{13}C)aminoethyl that was covalently attached to the protein via a thiol linkage, the single reactive thiol linkage in the protein being that of the K175C cysteine. Figure 5D shows an HSQC spectrum for aziridine-modified, exhaustively dialyzed cysteine-minus VP39 superimposed on a portion of Figure 3A. No signal was observed in this control spectrum corresponding to the $-S-CH_2-CH_2-NH_2$ chemical signature of covalently modified protein, reinforcing the above interpretation that the signature detected in Figure 5A−C is cysteine modification-specific.

The black line-connected peaks in the spectrum set of Figure 5 were plotted vs pH (Figure 6), and the apparent pK_a of the titratable group was deduced to be 8.507 (±standard deviation of 0.0687), representing a downward shift of greater than 1.6 and 2.4 p*K* units with respect to the control tripeptides AC_mW and AKW, respectively (Figure 3B and associated text). Apparent Hill coefficients for the ^{13}C and ^{1}H plots were 2.194 ± 0.20 (standard deviation) and −1.353 ± 0.152, respectively. These two values, although derived from the same spectra, appear to be distinct with a statistical certainty of ~99.15% (coinciding only at ~2.4 standard deviations from their respective means). We attribute differences between the coefficients to the difference

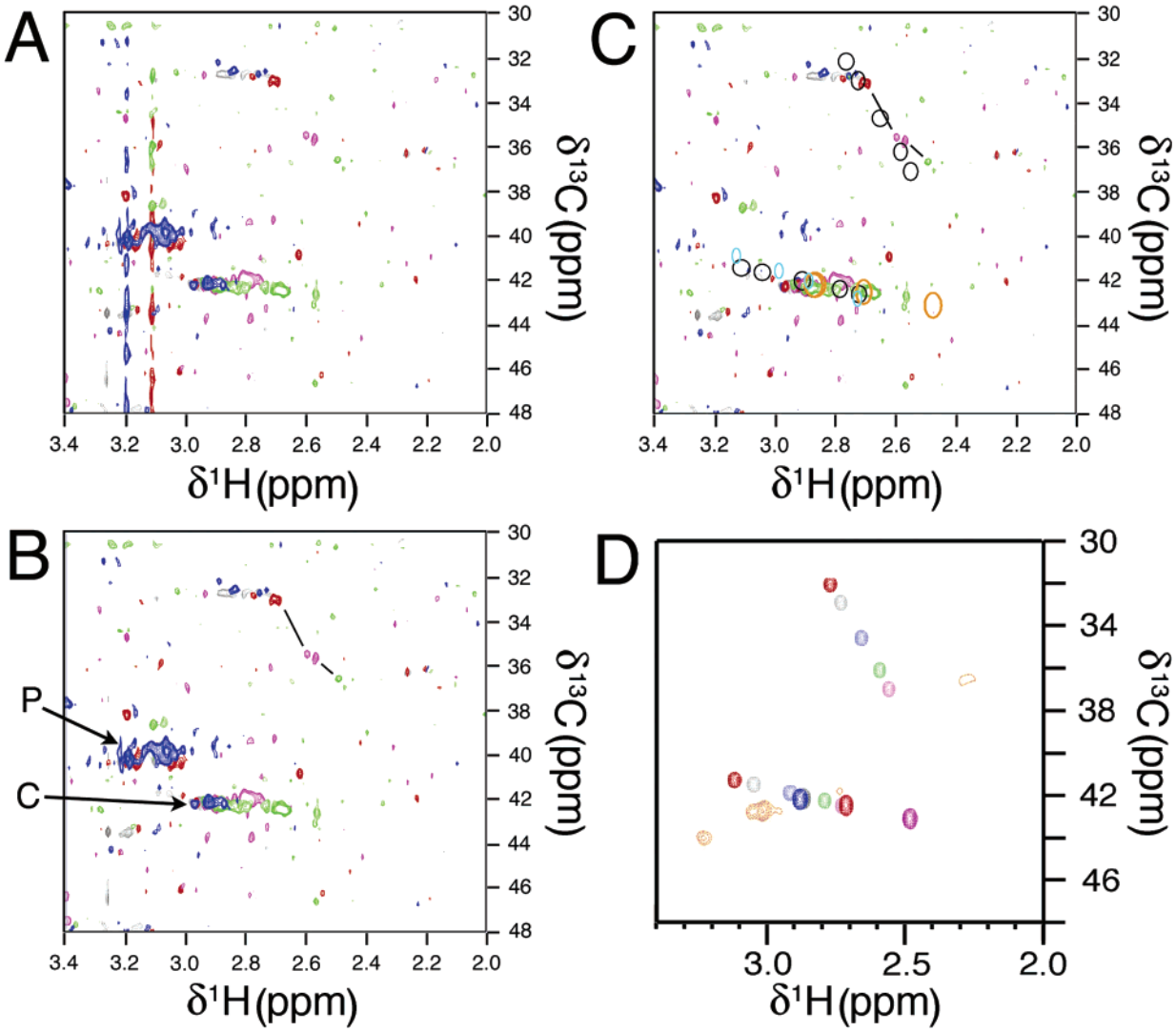

FIGURE 5: pH titration of (^{13}C)aziridine-modified VP39-C272S/K175C/R209K. (A) Overlaid spectra (unfiltered) taken at various points during the titration: pH 6.45 (black), 6.9 (blue), 7.8 (red), 9.0 (mauve), and 9.8 (green). (B) As in (A), after manual removal of foldback products. P is the signal identified as P in Figure 4C (residual polymer). The next most abundant signals after P and C appear to shift progressively with pH and are connected with black lines. (C) As in (B) except the P signal has been removed manually, and overlaid rings (black, orange, cyan) show positions of signals from AC_mW (carbons 5 and 6), AKW (δ carbon), and TETA (β carbon) pH titrations, respectively (positions transposed from Figure 3A). (D) Positions of signals from the control protein Cys-minus VP39 after modification and exhaustive chelating dialysis as above (HSQC were acquired at pH 6.4). HSQC NMR signals (orange) from the resulting material are shown overlaid on the plot of Figure 3A.

in accuracy with which δ could be read from the two dimensions of NMR plots, since the dispersion of ^{1}H signals was 12-fold less than that for ^{13}C and was therefore read with correspondingly lower accuracy (as reflected in the vertical error bars on the plots). Thus, the Hill coefficient for the titration appears to have a value greater than 1, perhaps around 2 (from the ^{13}C plot).

DISCUSSION

In a previous study, an orbital steering mechanism was proposed as the catalytic mechanism for *O*-methyltransferase enzymes (*17*), a mechanism that would require pK_a depression for the catalytic lysine in the context of intact enzyme. To address the pK_a of the catalytic lysine ϵ-amino group in situ, we used, as a model, the mRNA cap-specific RNA 2′-*O*-methyltransferase (VP39) from vaccinia virus and measured the apparent pK_a of the chemically rescued lysine directly by HSQC NMR. Although use of NMR techniques for direct measurements of lysine side chain pK_a in intact proteins has been documented (*35*), stable isotopes are typically incorporated in vivo using ^{13}C-enriched amino acids. In our case, however, it was felt that VP39's possession of 21 lysine residues would present insurmountable problems in the interpretation of spectra generated from in vivo labeled protein. To examine the pK_a of VP39's lysine 175, we substituted it with the analogue γ-thialysine, accompanied by site-specific ^{13}C enrichment, using a chemical modification rescue strategy. This was implemented by first making a serine substitution at the sole chemically reactive naturally occurring cysteine [C272S, a mutation that does not affect methyltransferase activity (*16*)], followed by a catalytically crippling K175C mutation at the catalytic center and restoration to enzymatic activity (Figure 2C) by chemical modification rescue.

The ^{13}C-enriched rescue reagent was shown to be covalently bound to the protein at the target cysteine, and the only clearly pH-responsive signal in subsequent HSQC experiments was spectrally positioned precisely as expected

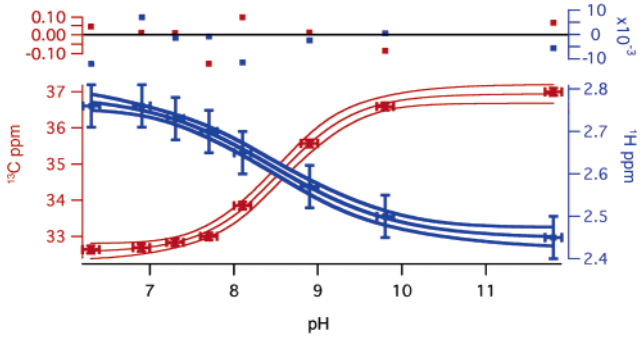

FIGURE 6: pK_a of γ-thialysine in the VP39 catalytic center. δ values for all pH points for carbon 6 (including the five shown in Figure 5A−C) are plotted vs pH. Vertical and horizontal error bars represent estimated error in quantifying $\Delta\delta$ and variation in pH during data acquisition, respectively. Sigmoidal curve fits area shown, flanked by additional curves representing statistical 95% confidence limits (number of fit iterations = 3 or 4). Residuals (shown above the curve fits) appear nonsystematic, indicating the appropriateness of the fitting equation used. Fitting to the ^{13}C and ^{1}H data yielded apparent pK_a values of 8.548 ± 0.0505 and 8.467 ± 0.0868 (standard deviation), respectively (mean = 8.507 ± mean standard deviation of 0.0687) for γ-thialysine covalently linked to VP39's catalytic center.

for an S-linked aminoethyl (according to tripeptide controls) and distinct from the spectral positions of noncovalently attached aziridine polymer. Moreover, the apparent pK_a of the site-specifically attached probe, in the context of the active enzyme catalytic center, was shown to be distinct from that of possible alternative compounds such as aziridine polymer. The methodology described here provides a gentle way to site-specifically modify a cysteine side chain to γ-thialysine in a native, ~40 kDa protein at ambient temperature and pH in such a way that it is subsequently possible to detect HSQC NMR signals from just two heavy atoms.

Aziridine has a propensity to slowly self-polymerize in aqueous solution or in the presence of trace amounts of water (*29*−*31*). Moreover, covalent incorporation of self-polymer at cysteinyl residues could be envisioned due to the presence at the terminus of the polymer of, for example, an intact aziridine moiety (*31*, *36*). In prior studies employing the Cys → Lys chemical modification rescue of enzyme activity (*1*, *4*, *8*, *10*, *14*), noncovalently and covalently attached self-polymer would typically be silent, affecting perhaps only specific activity rather than activity per se. However, covalently labeling with aziridine followed by monitoring of signals from the correctly attached modifying group present at only a single copy per protein molecule, required (a) the fastidious removal of ^{13}C-enriched side products that were not covalently attached to the protein such as aziridine self-polymer, (b) the removal of organics at natural ^{13}C-isotopic abundance but higher molecular abundance, and (c) the earmarking of lower abundance material that could not be removed, such as very tightly noncovalently bound or misdirected covalent adducts.

As a precaution against self/side-reaction products that could form during aziridine storage, only the freshly synthesized compound was used for protein modification. Although the extent of aziridine self-polymerization during the protein modification reaction was unclear (it was not assayed directly), very strong HSQC signals were eliminated via a chelating dialysis step included after protein modification but prior to NMR spectroscopy. This step was designed to strip the protein of noncovalently (electrostatically) adsorbed self-polymer, exploiting the chelating properties of PEI (the aziridine self-polymer expected to form preferentially). Ni^{2+} or Mn^{2+} was used in the dialysis buffer out of three considerations: solubility of trace amounts of metal phosphate, coordination efficiency of metal with the polymer, and stability of the metal salts at pH 8. Paramagnetic line broadening was minimized by dialysis against EDTA to remove traces of Ni^{+} or Mn^{2+}. Evidence that self-polymer had indeed formed during the protein modification reaction rested largely on preliminary experiments indicating the critical requirement for the metal ion/EDTA steps in the dialysis procedure in order to obtain a MALDI-TOF peak with bona fide *m*/*z* and also from HCCH COSY NMR experiments with undialyzed protein, which showed strong signals corresponding to aziridine dimer and trimer (data not shown). The chelating dialysis-dependent diminution or complete abrogation of a number of prominent HSQC peaks attested to the efficacy of this step. Fortuitously, only trace amounts of higher order polymer were detected covalently attached to the protein (as indicated by the mass spectrometric characterization of tripeptide and protein modification products; Figures 2B and 4C and data not shown). This indicated a suppression of the more reactive, aziridine-terminated form of the self-polymer in either abundance or cysteine thiol reactivity or both. The almost complete absence of higher order covalent protein adducts of aziridine simplified the interpretation of HSQC spectra.

According to an orbital steering model for activation of VP39's methylation target, namely a 2′OH of its mRNA substrate (*17*), a deprotonated form of VP39's catalytic lysine (K175) stabilizes and forms a hydrogen bond with the 2′OH proton such that a free 2′OH oxygen orbital points directly at the cofactor methyl group (*17*). VP39's methyltransferase activity exhibits a bell-shaped pH profile, whose optimum is at pH 7.5 (*37*) or 8.0 (*18*) and whose downward arm has been shown to correspond to a weakening of substrate binding (*18*). It seems reasonable to suppose that the upward arm [pH 6.5−8.0 (*18*) or 6.75−7.5 (*37*) with its inflection around pH 7.1−7.25] represents activation (deprotonation) of the catalytic lysine, and this inflection may therefore represent the pK_a of K175 in wild-type VP39. Since the pK_a for the side chain Nϵ of free lysine in water is ~10.5, such a pK_a for lysine would represent a pK_a depression of ~3 pH units in the context of VP39's 3D structure with respect to free lysine. Depressed pK_a values for lysine side chains in the context of intact proteins are not uncommon, however. They may result from a hydrophobic side chain microenvironment (*38*−*40*). Calculations indicate that only 0−12% of K175's overall surface area is solvent-exposed (depending upon the parameters used to calculate solvent exposure; data not shown), though the Nϵ atom of K175 appears to be entirely solvent-exposed (Figure 7A). Microenvironmental hydrophobicity may therefore play only a limited role in depressing K175's amino pK_a.

A low lysine pK_a can also arise from electrostatic factors (*40*), in which the proximity of a "like" charge (such as the side chain of an arginine or another, adjacent lysine) can increase the lysine amino group's tendency to deprotonate in order to relieve the electrostatic repulsion (*41*). Scrutiny of the VP39 crystal structure indicates that, in the wild-type

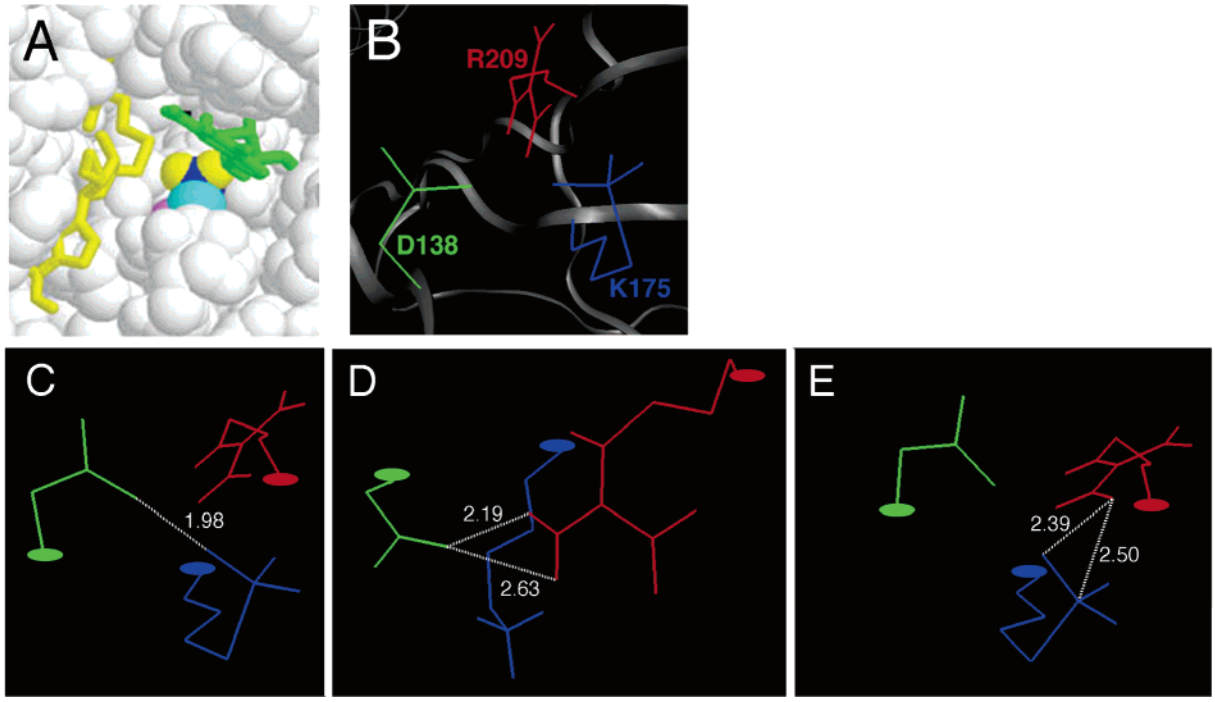

FIGURE 7: (A) Space-filling model of VP39 showing a view into the methyltransferase catalytic center. The K175 side chain is colored: blue, Nϵ; yellow, Nϵ amino protons; cyan, Cϵ; mauve, Cδ. The *S*-adenosylhomocysteine cofactor and the target nucleotide (stick representation) are colored yellow and green, respectively. (B) VP39's catalytic triad; the two side chains at the VP39 catalytic center located closest to K175. (C−E) For the side chains of K175, D138, and R209, bond distances are shown for individual pairs D138−K175, D138−R209, and K175−R209, respectively. In each panel, the triad has been reorientated for clarity of bond representation and labeling.

enzyme, the side chains of two residues, D138 and R209, are within closest hydrogen-bonding distance of K175's side chain amino group (Figure 7B), 1.98 and 2.39 Å, respectively (Figure 7C,E). The partially sp^2-hybridized (i.e., planar) terminal moieties of both of these side chains are almost precisely perpendicular to one another (Figure 7B−E), with R209's orbitals orientated perpendicularly to the orbitals of both D138 and K175 (Figure 7B,C) but with D138's orbitals orientated in a manner conducive to hydrogen bond formation with K175. Specifically, the H atoms of K175's Nϵ can be swiveled almost directly across an orbital of one of the two D138 carboxyl oxygens. Evidence for a strong bond between K175 and an opposite charge such as that of D138 comes from the Hill coefficient for the K175 titration, which appeared to be significantly greater than unity, perhaps approaching a value of 2.0 (see Results).

We suggest that the effect exerted by the R209 side chain is purely electrostatic in nature with no direct hydrogen bonding, acting to repel an approaching proton and/or promote loss of a proton from K175 to relieve repulsion. Since the pK_a of the arginine side chain (12.5) is higher than that for lysine, the pK_a depression would be experienced primarily by the lysine. It may be argued that proximity of a negative charge (D138) would have the opposite effect, namely, stabilization of a proximal positive charge via salt-link formation, leading to an elevation of the lysine pK_a (*40*, *42*). However, since D138 and K175 are already ionized at physiological pH, perhaps the presence of the D138 negative charge does not provide a thermodynamic impetus to drive K175's pK_a upward. Instead, perhaps D138's role is to provide a strong hydrogen bond acceptor. A D138 carboxylate orbital may thus be "pulling" K175's proton away more avidly than it is creating an electrostatic environment to stabilize K175's protonated state. Overall then, K175's pK_a may be controlled by a combination of purely electrostatic effects (R209) and proton "pulling" effects (D138). To stably accept a proton, D138, in turn, would presumably need to have an elevated pK_a. Although there are no negatively charged side chains nearby to promote this, a hydrophobic environment might be a possibility.

The pK_a of 8.5 measured here for the thialysine side chain at position 175 was insufficiently depressed, by ~1.25 pH units, to fully account for the upward arm of VP39's 2′-*O*-methyltransferase pH profile. The protein studied here, however, was the VP39-R209K mutant. The measured pK_a may therefore be entirely consistent with enzyme function if the lysine substitution at position 209 recapitulates only a portion of the electrostatic potential of arginine, or if partial pK_a depression in the mutant was entirely attributable to D138. Studies to examine pK_a effects in D138 mutants, an R209A mutant and a protein that is wild type at both positions 138 and 209, are ongoing. Mutant R209A shows no methyltransferase activity (data not shown), consistent with a model whereby some positive charge at position 209 is essential.

The experimental system described here, in which electrostatic interactions can be individually dissected and the resulting pK_a effects assayed, could be developed further: For example, NMR signal:noise might be raised in a number of ways, such as by doing replicate titrations (perhaps along with replicate modification reactions) and then summing spectra. Recombinant protein could be produced in *E. coli* grown in the presence of D_2O to eliminate proton-coupling signals from ^{13}C at natural abundance. Moreover, an HCCH COSY experiment could be developed in which signals are acquired specifically from two adjacent ^{13}C atoms, which would be expected to be highly selective for the chemical probe employed, thereby rejecting natural abundance ^{13}C within the protein. Although the latter was tried, sensitivity

was insufficient even at very high scan number due to our inability to produce sufficiently concentrated protein. Certainly, a different buffer system or salt concentration may permit the production of more concentrated protein. Finally, the addition of some inhibitor to slow the polymerization of aziridine may lead to increased modification efficiency.

ACKNOWLEDGMENT

We thank Shi-Mei Wang for generating and testing VP39 mutant K175C, Youlin Xia and Bao Nguyen for help with NMR instrument operation, and Xiaolian Gao and Melanie Cocco for discussions on NMR spectroscopy.

REFERENCES

1. Smith, H. B., and Hartman, F. C. (1988) Restoration of activity to catalytically deficient mutants of ribulosebisphosphate carboxylase/oxygenase by aminoethylation, *J. Biol. Chem. 263*, 4921−4925.
2. Smith, H. B., Larimer, F. W., and Hartman, F. C. (1988) Subtle alteration of the active site of ribulose bisphosphate carboxylase/oxygenase by concerted site-directed mutagenesis and chemical modification, *Biochem. Biophys. Res. Commun. 152*, 579−584.
3. Planas, A., and Kirsch, J. F. (1990) Sequential protection-modification method for selective sulfhydryl group derivatization in proteins having more than one cysteine, *Protein Eng. 3*, 625−628.
4. Smiley, J. A., and Jones, M. E. (1992) A unique catalytic and inhibitor-binding role for Lys93 of yeast orotidylate decarboxylase, *Biochemistry 31*, 12162−12168.
5. Lorimer, G. H., Chen, Y. R., and Hartman, F. C. (1993) A role for the epsilon-amino group of lysine-334 of ribulose-1,5-bisphosphate carboxylase in the addition of carbon dioxide to the 2,3-enediol(ate) of ribulose 1,5-bisphosphate, *Biochemistry 32*, 9018−9024.
6. Kim, D. W., Yoshimura, T., Esaki, N., Satoh, E., and Soda, K. (1994) Studies of the active-site lysyl residue of thermostable aspartate aminotransferase: Combination of site-directed mutagenesis and chemical modification, *J. Biochem. (Tokyo) 115*, 93−97.
7. Salvucci, M. E., and Klein, R. R. (1994) Site-directed mutagenesis of a reactive lysyl residue (Lys-247) of Rubisco activase, *Arch. Biochem. Biophys. 314*, 178−185.
8. Gloss, L. M., and Kirsch, J. F. (1995) Decreasing the basicity of the active site base, Lys-258, of *Escherichia coli* aspartate aminotransferase by replacement with γ-thialysine, *Biochemistry 34*, 3990−3998.
9. Messmore, J. M., Fuchs, D. N., and Raines, R. T. (1995) Ribonuclease A: Revealing structure−function relationships with semisynthesis, *J. Am. Chem. Soc. 117*, 8057−8060.
10. Highbarger, L. A., Gerlt, J. A., and Kenyon, G. L. (1996) Mechanism of the reaction catalyzed by acetoacetate decarboxylase. Importance of lysine 116 in determining the pK_a of active-site lysine 115, *Biochemistry 35*, 41−46.
11. Nash, H. M., Lu, R., Lane, W. S., and Verdine, G. L. (1997) The critical active-site amine of the human 8-oxoguanine DNA glycosylase, hOgg1: Direct identification, ablation and chemical reconstitution, *Chem. Biol. 4*, 693−702.
12. Paetzel, M., Strynadka, N. C., Tschantz, W. R., Casareno, R., Bullinger, P. R., and Dalbey, R. E. (1997) Use of site-directed chemical modification to study an essential lysine in *Escherichia coli* leader peptidase, *J. Biol. Chem. 272*, 9994−10003.
13. Bochar, D. A., Tabernero, L., Stauffacher, C. V., and Rodwell, V. W. (1999) Aminoethylcysteine can replace the function of the essential active site lysine of *Pseudomonas mevalonii* 3-hydroxy-3-methylglutaryl coenzyme A reductase, *Biochemistry 38*, 8879−8883.
14. Harpel, M. R., Larimer, F. W., and Hartman, F. C. (2002) Multifaceted roles of Lys166 of ribulose-bisphosphate carboxylase/oxygenase as discerned by product analysis and chemical rescue of site-directed mutants, *Biochemistry 41*, 1390−1397.
15. Hopkins, C. E., O'Connor, P. B., Allen, K. N., Costello, C. E., and Tolan, D. R. (2002) Chemical-modification rescue assessed by mass spectrometry demonstrates that gamma-thia-lysine yields the same activity as lysine in aldolase, *Protein Sci. 11*, 1591−1599.
16. Schnierle, B. S., Gershon, P. D., and Moss, B. (1994) Mutational analysis of a multifunctional protein, with mRNA 5′ cap-specific (nucleoside-2′-O-)-methyltransferase and 3′-adenylyltransferase stimulatory activities, encoded by vaccinia virus, *J. Biol. Chem. 269*, 20700−20706.
17. Li, C., Xia, Y., Gao, L., and Gershon, P. D. (2004) Mechanism of RNA 2′-O-methylation: Evidence that the catalytic lysine acts to steer rather than deprotonate the target nucleophile, *Biochemistry 43*, 5680−5687.
18. Lockless, S. W., Cheng, H.-T., Hodel, A. E., Quiocho, F. A., and Gershon, P. D. (1998) Recognition of capped RNA substrates by VP39, the vaccinia virus-encoded mRNA cap-specific 2′-O-methyltransferase, *Biochemistry 37*, 8564−8574.
19. Kasermann, F., Wyss, K., and Kempf, C. (2001) Virus inactivation and protein modifications by ethyleneimines, *Antiviral Res. 52*, 33−41.
20. Ellman, G. L. (1959) Tissue sulfhydryl groups, *Arch. Biochem. Biophys. 82*, 70−77.
21. Markley, J. L. (1975) Observation of histidine residues in proteins by means of nuclear magnetic resonance spectroscopy, *Acc. Chem. Res. 8*, 70−80.
22. Sayle, R. A., and Milner-White, E. J. (1995) RASMOL: biomolecular graphics for all, *Trends Biochem. Sci. 20*, 374.
23. Humphrey, W., Dalke, A., and Schulten, K. (1996) VMD−Visual molecular dynamics, *J. Mol. Graphics 14*, 33−38.
24. Hodel, A. E., Gershon, P. D., and Quiocho, F. A. (1998) Structural basis for sequence non-specific recognition of 5′-capped mRNA by a cap modifying enzyme, *Mol. Cell 1*, 443−447.
25. Okazaki, K., Yamada, H., and Imoto, T. (1985) A convenient S-2-aminoethylation of cysteinyl residues in reduced proteins, *Anal. Biochem. 149*, 516−520.
26. Cole, R. D. (1967) S-aminoethylation, in *Methods in Enzymology*, pp 315−317, Academic Press, New York.
27. Raftery, M. A., and Cole, R. D. (1963) Tryptic cleavage at cysteinyl peptide bonds, *Biochem. Biophys. Res. Commun. 10*, 467−472.
28. Raftery, M. A., and Cole, R. D. (1966) On the aminoethylation of proteins, *J. Biol. Chem. 241*, 3457−3461.
29. Barb, W. G. (1955) Some aspects of the polymerization and depolymerization of N-substituted ethyleneimines, *J. Chem. Soc., Abstr.*, 2577−2580.
30. Barb, W. G. (1955) The kinetics and mechanism of the polymerization of ethyleneimine, *J. Chem. Soc., Abstr.*, 2564−2577.
31. Nepomnyaschaya, N. M., Tsvetkova, E. A., and Strelenko, Y. A. (2004) Oligoaziridines: ring opening with hydrobromic acid, *Mendeleev Commun.*, 1−2.
32. Hermann, V. P., and Lemke, K. (1968) Ionization constants and stability constants of copper (II) complexes of some amino acids and their sulfur-containing analogs, *Hoppe-Seyler's Z. Physiol. Chem. 349*, 390−394.
33. Shi, X., Bernhardt, T. G., Wang, S.-M., and Gershon, P. D. (1997) The surface region of the bifunctional vaccinia RNA modifying protein VP39 that interfaces with poly(A) polymerase is remote from the RNA binding cleft used for its mRNA 5′ cap methylation function, *J. Biol. Chem. 272*, 23292−23302.
34. Oguro, A., Johnson, L., and Gershon, P. D. (2002) Path of an RNA ligand around the surface of the vaccinia VP39 subunit of its cognate VP39−VP55 protein heterodimer, *Chem. Biol. 9*, 679−690.
35. Damblon, C., Raquet, X., Lian, L. Y., Lamotte-Brasseur, J., Fonze, E., Charlier, P., Roberts, G. C., and Frère, J. M. (1996) The catalytic mechanism of beta-lactamases: NMR titration of an active-site lysine residue of the TEM-1 enzyme, *Proc. Natl. Acad. Sci. U.S.A. 93*, 1747−1752.
36. Dermer, O. C., and Ham, G. E. (1969) in *Ethyleneimine and other aziridines*, pp 327−333, Academic Press, New York.
37. Barbosa, E., and Moss, B. (1978) mRNA(nucleoside-2′-)-methyltransferase from vaccinia virus: Characteristics and substrate specificity, *J. Biol. Chem. 253*, 7698−7702.
38. Barbas, C. F., Heine, A., Zhong, G., Hoffmann, T., Gramatikova, S., Bjornestedt, R., List, B., Anderson, J., Stura, E. A., Wilson, I. A., and Lerner, R. A. (1997) Immune versus natural selection: Antibody aldolases with enzymic rates but broader scope, *Science 278*, 2085−2092.

39. Dao-pin, S., Anderson, D. E., Baase, W. A., Dahlquist, F. W., and Matthews, B. W. (1991) Structural and thermodynamic consequences of burying a charged residue within the hydrophobic core of T4 lysozyme, *Biochemistry 30*, 11521−11529.
40. Harris, T. K., and Turner, G. J. (2002) Structural basis of perturbed pK_a values of catalytic groups in enzyme active sites, *IUBMB Life 53*, 85−98.
41. Westheimer, F. H. (1995) Coincidences, decarboxylation, and electrostatic effects, *Tetrahedron 51*, 3−20.
42. Slilaty, S. N., and Vu, H. K. (1991) The role of electrostatic interactions in the mechanism of peptide bond hydrolysis by a Ser-Lys catalytic dyad, *Protein Eng. 4*, 919−922.

BI051736H